A comparison of three preprocessing techniques for kidney stone segmentation in CT scan images

Nilar Thein.
Universitas Gadjah Mada
Grafika 2 Street Yogyakarta 55281, Indonesia
nilarthein.mti13@mail.ugm.ac.id

Kazuhiko Hamamoto
Tokai University
Tokyo, Japan
hama@keyaki.cc.u-tokai.ac.jp

Hanung Adi Nugroho.
Universitas Gadjah Mada
Grafika 2 Street Yogyakarta 55281, Indonesia
adinugroho@ugm.ac.id

Teguh Bharata Adji
Universitas Gadjah Mada
Grafika 2 Street Yogyakarta 55281, Indonesia
eadji@ugm.ac.id

***Abstract*—Accurate segmentation techniques used in the automatedkidney stone detection is one of the most challenging problems because of grey levels similarities of adjacent organs, variation in shapes and positions of kidney stone. Valuable image preprocessing is an essential step to improve the performance of region of interest (ROI) segmentation by removing unwanted region (non ROI), noise and disturbance. The research aims to conductcomparative study of the three different preprocessing techniques for the noise removal from the CT image ofkidney stone. Three noise removal techniques are computed based on the size-based thresholding (method I), shape-based thresholding(method II) and hybrid thresholding algorithm (method III). The methods aim to enhance their readability and to assist the segmentation process in the kidney stone diagnosis system. Digitized transverse abdomen CT images from 75 patients with kidney stone cases were done in statistical analysis and validation. The estimation of coordinate points in the stone region was measured independently by the expert radiologists to get the validation data for the analysis. The results show that the proposed methodI, II and III havea sensitivity of 90.91%, 92.93% and 68.69%, respectively. The execution times of overall process were9.44 sec, 10.14 sec and 34.5 in average, respectively.**

Keywords— comparative study of preprocessing algorithms, intensity-based thresholding, size-based thresholding, shape-based thresholding , hybrid thresholding.

I. INTRODUCTION

Kidney stone formation is characterized by the formation of crystals in the kidney, ureter, bladder and urethra. All kidney stone problem can be recovered, and yet, the majority of stone cases are impossible to detect except in case when extreme abdominal pain is happened or abnormal urine color is noticed. Most of kidney stone case exhibit stone recurring after stone formation. Both of kidney stone problems (presence case and recurrence case) may causefailure of kidney function, until the death of kidney and implications on the degrees of chronic kidney disease (CAD). A potential risk factor of chronic kidney disease is the recurrent kidney stones forming associated with significant morbidity, mortality and heath care cost [1]. In GBD (GLOBAL BURDEN OF DISEASES) 2010, years of life lost (premature mortality) in chronic kidney disease has been increased to 50% over a period of 20 years (from 1990 to 2010) [2]. According to WHO data published in 2017, CAD death rate in Myanmar was 26.20 per 100 000 of population with the rank of 37 in the world while Indonesia and Japan were ranked 54 and 137 in the world [3]. Moreover, recurrence rate of renal stone in Myanmar is 14 % at one year after first stone while 10% at one year in other abroad and India [4][5]. Therefore, kidney stone problem becomes one of the most commonly reported problems among patients in Myanmar, due to nature of living.

Computed tomography (CT) is widely accepted as a gold standard imaging modality for kidney stone diagnosis. But, interpretation of CT scan is a time consuming task and mainly rely on the skill of radiologists[6]. Thus, advances in CT technology are being convenient and efficient in the kidney stone detection [7]. The CT imaging diagnostic system involves mainly of preprocessing, segmentation, feature extraction and classification. The output of each stage is the input of the next stage. Preprocessing, the most fundamental stage of diagnosis, either canaffect on misleading the results or can improve the performance of the system. Therefore, the achievement of diagnosiscritically relies on preprocessing stage [8]. Hence, in this study, the different image preprocessing scheme for kidney stone segmentation are compared based on their ability to remove noise and time of computation.

II. MATERIALS AND METHODS

A. CT image acquisition

CT images of kidney stone from 75-patients were used as the datasetwhich were performed using a Toshiba Aquilion 64-slice CT Scanner at No_2, Military Hospital, Yangon, Myanmar. The number of slices per patient ranges from 500 slices to 600 slices.Every cross-sectional slice is a two-dimensional image of 512 ×512 matrix size and 1 mm slice thickness, these are called the x-,y- and z- dimensions respectively.

B. Image preprocessing

Image preprocessing is a kind of image processing method at lowest level of concept. The aim of image preprocessing is to remove the unwanted and irrelevant data from the image and to enhance the features of the image for processing. The main task of preprocessing in kidney stone detection is to remove the noise and unneeded region from the abdominal CT image. There are two common approaches in image preprocessing, increasing the contrast of suspicious areas (contrast enhancement technique) and removing background noise (noise reducing technique).

978-1-5386-5724-9/17/$31.00 ©2018 IEEE

Fig. 1. Kidney stone in CT slice.

In this study, noise removing technique was approached and a comparative study wascarried out to investigate the effect of preprocessing techniques on kidney stone CT imaging. Three noise removal techniques were computed based on area-based thresholding, shape-based thresholdingand hybrid thresholdingalgorithm. Finally, their performance had been compared based on the sensitivity and computational time.

III. Proposed Methods

In order to investigate and implement allthe proposed methods, the available dataset and MAILAB computing were used for implementation. It could be seen many organs in abdominal, such as soft organs (stomach, gallbladder, intestines, liver, pancreas and spleen), hard organs (kidney stone and bones) and blood vessels in Fig. 1. Therefore, removing unneeded disturbance from CT images was basically one of the critical tasks in image segmentation. In this study, the pre-processing method was focused on removing the unneeded disturbance of the input DICOM image. All proposed methodsconsist of two major steps: Soft-organ removing and unneeded hard-organ removing.Theflow diagram in Fig. 2 describesthe process of three proposed noise removal techniques. And, the detailed description of each method is as follow.

A. Soft-organ removing

Among the proposed methods, only intensity-based thresholdingwas used to remove soft organs from the input abdominal CT image. A strength of CT image is its ability of the significant intensity (Hounsfield scale) differences between soft organs and hard organs. Soft organs have low intensity values while the others have high intensity values.Moreover, the HU values of kidney stones is varied in the

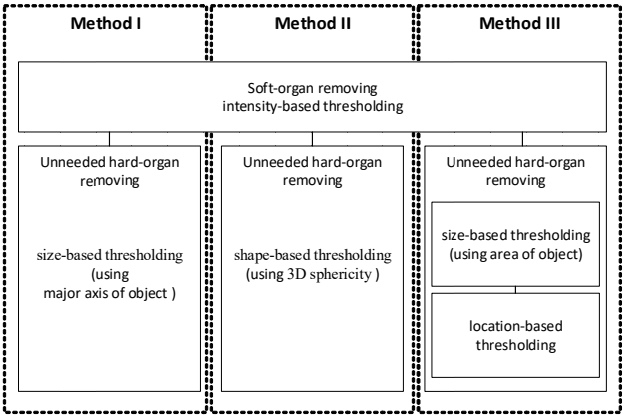

Fig. 2. Flowchart of three proposed methods for noise removal preprocessing

range between 200 HU to 2800 HU [9][10].Therefore, the soft organs in the image were removed by using intensity-based thresholding with two threshold value,$T_a$andT_b.

- Step 1, Select two constant threshold values, T_a and T_b, manually.

$$g(x,y) = \begin{cases} 1, & if T_a \le g(x,y) \le T_b \\ 0, & if\ else \end{cases} \quad (1)$$

where, T_a andT_b are regarded with 200 HU and 2800 HU, according to the kidney stone's HU value range.

- Step 2, Segment the image into two group of pixels $g(x,y)_1$ and $g(x,y)_2$, using T_a and T_b:
- Step 3, Develop the new image with $g(x,y)_1$, and without $g(x,y)_2$,

B. Unneeded hard-organ removing

After removing soft organs from the images, there were still many high-intensity regions left such as bed-map, bones, stones and noise. Therefore, a comparative study on three noise removal techniqueswas carried out in order to eliminate unneeded hard organs from the image. These three methods are described as follows.

I. *Method I:*

Kidney stones is available in a variety of sizes from the small-size as grain of sand until the large-size as golf balls (42.7mm)[11]. Therefore,we developed the first proposed noise removal method using the following size-based thresholding algorithm:

- Step 1, Calculate the size (longest diameter)of each 3D object in the image using "getSize_new" function in [12].
- Step 2, Select two constant threshold values, $L_{\min}$ and $L_{\max}$, manually, where, they are manually regarded with 3 mm and 50 mm diameter as consideration of general kidney stone size in [11].
- Step 3, Segment the image into two group of pixels$g(x,y)_1$ and without $g(x,y)_2$using , $L_{\min}$ and $L_{\max}$

$$g(x,y) = \begin{cases} 1, & if L_{min} \le g(x,y) \le L_{max} \\ 0, & if\ else \end{cases} \quad (2)$$

- Step 4, Develop the new image with $g(x,y)_1$,

II. *Method II:*

Sphericityis an important morphological feature to measure 3D shape parameter of kidney stone. This section presents the second noise removal techniques with the consideration of 3D sphericity of kidney stone. The shape of kidney stones is usually range in sphericity value between 0 and 1[13][14][15]. Therefore, the second methodwas developed using shape-based thresholding based on sphericity. The description of the second noise removal technique is presented as follows.

Step 1: Finding 3D object in the image

Using *the bwlabeln*function in MATLAB, the adjacent voxels in the image are connected to perform the connected-component cluster. These connected-components are labeled to identify voxels of each 3D object in the image.

Step 2: Finding the sphericity of 3D object in the image

Sphericity of the object expresses the irregularity of the shape of the object with certain degree of roundness. Sphericity of 3D object can be calculated if its surface area and volume are known [13][14][15]. A perfect sphere consequently has a sphericity value of 1. The sphericity value approaches zero if the shape deviates from a perfect sphere. In order to calculate the sphericity of object, the volume and surface area of object are formulated. In this study, we enhance the surface area and volume of 3D object from perimeter of 2D ROI in each slice as shown in Fig .3. Firstly, the surface area of 3D object was calculated as following algorithm.

- Step 1: Calculate the number of voxel at perimeter of ROI in each slice, S_i (using MATLAB*regionprops*function), and it is described asP_i.
- Step 2: Find the perimeter of an object by summing the number of voxel from all of ROI perimeters in an object, in equation (3).

$$P_{total} = \sum_{i=1}^{n} P_i \tag{3}$$

Where n is the number of slices where region of interest (ROI) is detected, P_i means the number of voxel at perimeter of ROI in each sliceS_i.

- Step 3: Calculate the surface area of 3D object by multiplying the total perimeter of an object and area of a voxel, in equation (4) and (5).

$$Surface\ Area\ of\ an\ object\ (SA) = P_{total} \times VoxelArea \tag{4}$$

$$Voxel\ Area = Voxel\ resolution\ \times Slice\ spacing \tag{5}$$

And then, the volume of 3D object was calculated as following algorithm.

Step 1: Calculate the area of ROI in each slice, S_i (using *regionprops*function), and it is described as A_i.

Step 2: Find area of an object by summing all ROI area of slices of an object, in equation (6).

$$A_{total} = \sum_{i=1}^{n} A_i \tag{6}$$

Where n is the number of slices where region of interest (ROI) is detected; A_i means the area of ROI in each slice.

Step 3: Calculate the volume of 3D object by multiplying the total ROI area with resolution of voxel in the X, Y and Z direction, in equation (7).

$$Volume\ of\ an\ object = A_{total} \times res_x \times res_y \times res_z \tag{7}$$

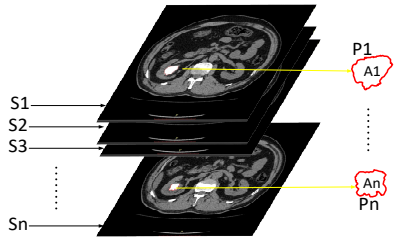

Fig. 3. Area and perimeter estimation for each slice S_i.

Using surface area and volume of the above equations, the sphericity of object can be calculated using in equation (8).

$$Sphericity = \frac{\sqrt[3]{36 \times \pi \times V^2}}{SA} \tag{8}$$

where$V$ and $SA$are the volume and surface area of 3D object.

Finally, shape-based thresholdingwas used for the second noise removal techniques as following algorithm:

- Step 1, Calculate the sphericity of each 3D object in the image using equation (8):
- Step 2, Select two constant threshold values, $Sph_{\min}$and$Sph_{\max}$. Where, $Sph_{\min}$ and $Sph_{\max}$ are manually regarded with 0 and 1 as consideration of sphericity of kidney stone in [13][14][15].
- Step 3, Segment the image into two groups of pixels $g(x,y)_1$ and without $g(x,y)_2$using,$Sph_{\min}$and$Sph_{\max}$,in equation (9).

$$g(x,y) = \begin{cases} 1, & if Sph_{\min} \le g(x,y) \le Sph_{\max} \\ 0, & if\ else \end{cases} \tag{9}$$

- Step 4, Develop the new image with $g(x,y)_1$,

III. Method III

In the third proposed technique, the unwanted regions could be removed by using two thresholding algorithms based onsize and location.

Finding the largest object in the imagecan eliminate the bony skeleton (a group of rib cage, vertebral column and pelvic cage) because it is the largest object among all of objects in the image. Therefore, to eliminate bony skeleton, we developed the following size-based thresholding algorithm:

- Step 1, Calculate the area of each 3D object in the image using MATLAB *regionprops'* function:
- Step 2, Find the maximum object area $O_{\max}$ using MATLAB '*max'* function:
- Step 3, Segment the image into two group of pixels $g(x,y)_2$ and without $g(x,y)_1$ using $O_{\max}$, in equation (6),

$$g(x,y) = \begin{cases} 0, & if O_{\max} = g(x,y) \\ 1, & if\ else \end{cases} \tag{10}$$

- Step 4, Develop the new image with $g(x,y)_2$,

And then, estimating the location of kidney stone region could remove bed-mat and reduce the noise in the image. As the consideration of the nature of CT scanning, kidney

stones are existed in the enclosed region of the bonyskeleton and bed-mat is located at the behind of bony skeleton in Fig 4.

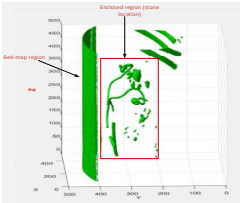

Fig. 4. Location of bed-map, stone and bones on CT

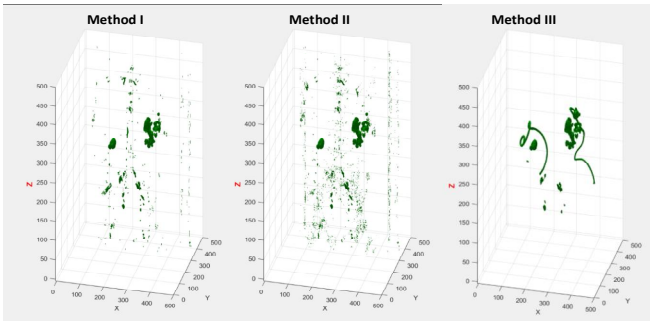

Fig. 5. Visualization result of all three proposed preprocessing methods

Therefore, to eliminate bed-mat, we developed the following location-based thresholding algorithm:

- Step 1, Estimate two coordinate points with X, Y and Z direction manually, $Corr_{xyz-1}$ and $Corr_{xyz-2}$:
- Step 2, Segment the image into two group of pixels $g(x,y)_1$ and without $g(x,y)_2$ using $Corr_{xyz-1}$ and $Corr_{xyz-2}$, in equation (11):

$$g(x,y)=\begin{cases}1, & \text{if} Corr_{xyz\text{-}1} \le g(x,y) \le Corr_{xyz\text{-}2} \\ 0, & \text{if else}\end{cases} \quad (11)$$

- Step 4, Develop the new image with $g(x,y)_1$.

The proposed location-based thresholdingcan performnot only bed-mat removingbut also noise (is located in front of the bony skeleton) reduction. Although the proposed method was not robust, it could completely remove bed-mat with noise reduction as shown in Fig .5.

IV. Results And Discussion

A. Data Analysis and Prototype Application

Data analysis for this study was tested on abdominal CT images which were based on the incidence of kidney stone. The experiments were carried out on a PC with Intel(R) Core(TM) i7-7700HQ CPU @ 2.80 Hz, 8 GByte of RAM, and the computations were performed under MATLAB 9.0 (R2016a). From the dataset contained 75 patients, CT scan image with DICOM format were used for testing. As a reference manual detection, estimation of coordinate points in stone region was created by expert radiologist. We computed our preprocessing with the reference detection to evaluate our methods.

B. Result Analysis

Experiments were performed and verified with the dataset included 75 patients.

1) 3D Visualization

Visualization in CT scan imaging is an important aspect of kidney stone diagnosing. Working on 551 slices of abdominal CT image of a patient No-9, visualization analysis of this study was carried out. The experimental results in Fig .6, is a demonstration of original slice mode and the volume mode of the proposed soft-organ removing method. The slise mode is presented some slices of original DICOM image from patient No-9. 3D volume mode is the result of all three proposed methods after soft-organ removing.

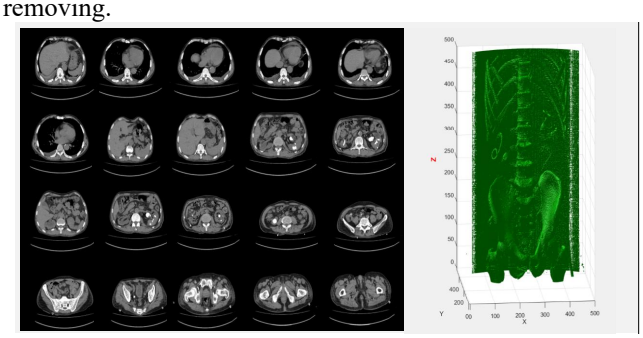

Fig. 6. Slice mode of original DICOM image and volume mode of soft-organ removing result

This experiment show that intensity-based thresholding of proposed methods can completely remove all soft organs in the abdominal CT image. After unneeded hard organ removing, the results of all three proposed methods are different.The figures in left, middle and right of Fig .5. are the resulted image of each proposed preprocessing method, I, II and III, respectively.

According to the result, they can remove many high intensity regions such as the bony skeleton, bed-mat.But, there was still some remain items in the image, bed-map, stone, stent and other fragmented bones. Among these analysis, the performance of method III is better than other methods because it can produce 3D output image with lowest disturbance.

2) Time analysis

For time analysis of this study, it was carried out a comparison of processing time for three proposed methods as shown in Fig .7. There was no significant difference in processing times between method I and II which took about 9.44 seconds and 10.14 seconds in average of a whole dataset. But, method III took over three times slower than other two methods and its average processing time was 34.5 seconds.

3) Performance Evaluation

As an evaluation parameters, sensitivity, was used in this study for a comparison of proposed algorithms: In [16], it could be calculated using TP and FN rate as shown below:

$$Sensitivity = \frac{TP}{(TP+FN)} \quad (12)$$

TP is used for kidney stone, which are correctly detected. FN is used for kidney stone, which are not detected.

The program output and manual record were arranged to valid the performance of all threemethods.The experimental result for stone detection is presented in Table I where

sensitivity is calculated using equation (12). Ability to detect and mark kidney stones of all three methods I, II

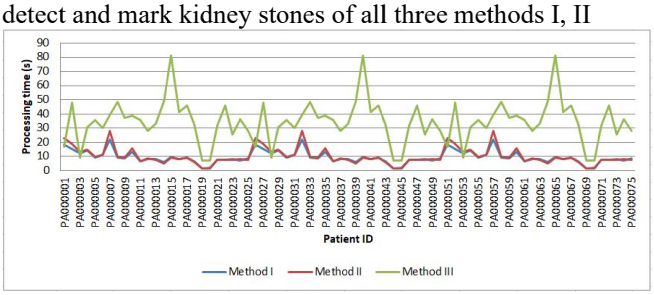

Fig. 7. A comparison of execution time for each proposed preprocessing method

TABLE I. A COMPARISON OF PERFORMANCE EVALUATION FOR THREE PROPOSED METHODS

Method	TP	FP	Sensivity
I	90	9	90.91%
II	92	7	92.93%
III	68	31	68.69%

and III were 90.91%, 92.93% and 68.69%, in sensitivityrespectively. It is found that these methods work unneeded regions removing with a significant true positive (stones) detecting. It gives a clear output image for segmentation although there are still remain false positive.Especially, the accuracy of method II resulted in a sensitivity of 92.93% which is the highest value compare with other two methods.

V. CONCLUSION

In this study, three preprocessing schemes using difference thresholding methods were mentioned and their results were compared. In general, they are simple and easy to understand for segmentation. Moreover, the proposed thresholding methods correctly remove the unneeded region and provide the output image in a clear form. When comparing their performance in detail, method I and II have no significant difference in their process execution time and sensitivity value. But, method I can remove unneeded region more than method II and method II is better in sensitivity. Among all three methods, method III can remove unneeded region more than other. But its sensitivity value (68.69%) is about 30% lower than the other two methods and it execution time is over three times longer than others. According to our experimental results, method II is better and more satisfactory than other two methods because of its high sensitivity value (92.93%) with suitable execution time (10.14 seconds in average). As limitation, all proposed schemes are weak in robustness because they are completely dependent on the prior knowledge of the input image. Thus, we plan to explore more robust preprocessing process and to develop the accurate method for kidney stone segmentation.

.

ACKNOWLEDGMENT

The authors wish to acknowledge to the ASEAN University Network Southeast Asia Engineering Education Development Network (AUN/SEED-Net) program and JICA (Japanese International Cooperation Agency) for financial support.

REFERENCES

[1] A. H. Milladipour and M. Rezaei Hemami, “Renal Function Assessment in Adults with Recurrent Calcium Kidney Stone Disease,” *J. Nephrol. Ther.*, vol. 2, no. 4, pp. 2–4, 2012.

[2] YLDs, “WHO-Health metrics_GBD profile: Myanmar,” vol. 2010, no. Gbd, pp. 1–4, 1990.

[3] “SUPPORT LIFE EXPECTANCY RESEARCH!,” *WORLD HEALTH ORGANIZATION 2017*, 2017. [Online]. Available: http://www.worldlifeexpectancy.com/myanmar-kidney-disease.

[4] A. Soe, “KIDNEYS : A PAIR OF VITAL ORGANS ESSENTIAL FOR LIFE,” *The Global New Light of Myanmar*, vol. II, no. 324, pp. 8–9, 2016.

[5] “Chapter II Brief Review on Urinary Calculi,” in *GROWTH AND CHARACTERIZATION OF STRUVITE AND RELATED CRYSTALS*, 2011, pp. 28–112.

[6] S. G. Armato, M. L. Giger, C. J. Moran, J. T. Blackburn, K. Doi, and H. MacMahon, “Computerized detection of pulmonary nodules on CT scans,” *Radiographics*, vol. 19, pp. 1303–11, 1999.

[7] S. Ebrahimi and V. Y. Mariano, “Image Quality Improvement in Kidney Stone Detection on Computed Tomography Images,” *J. Image Graph.*, vol. 3, no. 1, pp. 40–46, 2015.

[8] U. Jamil, “Valuable Pre-processing & Segmentation Techniques Used in Automated Skin Lesion Detection Systems,” pp. 290–295, 2015.

[9] Y. Andrabi, M. Patino, C. J. Das, B. Eisner, D. V Sahani, and A. Kambadakone, “Advances in CT imaging for urolithiasis.,” *Indian J. Urol.*, vol. 31, no. 3, pp. 185–93, 2015.

[10] G. Chevreau *et al.*, “Estimation of urinary stone composition by automated processing of CT images .,” pp. 1–11.

[11] N. Kidney, U. Diseases, and I. Clearinghouse, “Kidney Stones in Adults,” *NIH Publ.*, vol. 13–2495, no. February 2013, pp. 1–12, 2012.

[12] M. Vallières, C. R. Freeman, S. R. Skamene, and I. El Naqa, “A radiomics model from joint FDG-PET and MRI texture features for the prediction of lung metastases in soft-tissue sarcomas of the extremities,” *Phys. Med. Biol.*, vol. 60, no. 14, pp. 5471–5496, Jul. 2015.

[13] B. Ã. Zhou, J. Wang, and H. Ã. Wang, “Three-dimensional sphericity , roundness and fractal dimension of sand particles,” no. 1, pp. 18–30, 2018.

[14] A. K. Dhara, S. Mukhopadhyay, A. Dutta, M. Garg, and N. Khandelwal, “A Combination of Shape and Texture Features for Classification of Pulmonary Nodules in Lung CT Images,” *J. Digit. Imaging*, vol. 29, no. 4, pp. 466–475, 2016.

[15] T. Paulose, M. Montévil, L. Speroni, F. Cerruti, C. Sonnenschein, and A. M. Soto, “SAMA: A method for 3D morphological analysis,” *PLoS One*, vol. 11, no. 4, pp. 1–14, 2016.

[16] W. Zhu, N. Zeng, and N. Wang, “Sensitivity, specificity, accuracy, associated confidence interval and ROC analysis with practical SAS implementations.,” *Northeast SAS Users Gr. 2010 Heal. Care Life Sci.*, pp. 1–9, 2010.